Journal of Applied Polymer Science

Highly luminescent film functionalized with CdTe quantum dots by layer-by-layer assembly

Zhenshun Li,[1,2,3] Shaolong Wan,[1] Wei Xu,[1] Yuntao Wang,[1] Bakht Ramin Shah,[1] Weiping Jin,[1] Yijie Chen,[1,4] Bin Li[1,4]

[1]College of Food Science and Technology, Huazhong Agricultural University, Wuhan 430070, China
[2]College of Life Science, Yangtze University, Jingzhou 434025, China
[3]Jingchu Food Research and Development Center, Yangtze University, Jingzhou 434025, China
[4]Key Laboratory of Environment Correlative Dietology, Huazhong Agricultural University, Ministry of Education, Wuhan 430070, China
Correspondence to: B. Li (E-mail: libinfood@mail.hzau.edu.cn)

ABSTRACT: Robust and facile strategies are required to fabricate film with high luminescence for application in the fields of biomaterials. In this study, the luminescent electrospinning cellulose fibrous mats were decorated with CdTe quantum dots (QDs) and poly(-diallyl dimethyl ammonium chloride) (PDDA) using layer by layer (LBL). The characterizations of the LBL films coated mats were executed by X-ray photoelectron spectroscopy, Fourier transform infrared spectroscopy, scanning electron microscopy, fluorescent spectroscopy, X-ray diffraction, thermal gravimetric analysis, and differential scanning calorimetry. The luminescent intensities were linearly increased with adding the amount of deposited bilayers. The green fabricated $(QDs/PDDA)_n$ coated mat through physical interactions is a promising luminescent material. © 2015 Wiley Periodicals, Inc. J. Appl. Polym. Sci. **2015**, *132*, 41893.

KEYWORDS: biomaterials; cellulose and other wood products; electrospinning; fibers; films

Received 17 August 2014; accepted 13 December 2014
DOI: 10.1002/app.41893

INTRODUCTION

Quantum dots (QDs), one of the most common semiconductive nanocrystals, are gaining a growing interest among researchers because of their high luminescence, low photobleaching, size-dependent optical character, and so on.[1,2] QDs are widely applied as light emitting diodes,[3–5] bioprobes in sensing,[6,7] imaging,[8–10] and other emitting materials.[11–13] In most applications, such as light emitting diodes and photoelectric biosensors, QDs are ultimately required to be stably immobilized on substrates such as films, which can effectively eliminate the issue of colloid diffusion.

Generally, the approaches of fabricating polymer/QDs thin films include QDs deposited on polymers by layer-by-layer (LBL), in situ synthesis QDs on polymers[14,15] and self-assembly of block copolymer, in which the QDs were incorporated into polymer matrix.[16–20] In these methods, LBL is the most versatile protocol to create thin films with controllable luminescent intensity, morphology, thickness, and so on.

In these days, electrospinning is becoming a versatile technique to fabricate thin films because it enables the nanofiber mat bearing various desired functionalities from a wide range of materials, such as polymers, sol-gels, polymer blends, and so on.[21] Moreover, compared with spin-coating films or quartz, electrospun films possess high surface area because of the three-dimensional ultrathin fiber structure. Therefore, electrospinning is a superior technique for creating luminescence thin films. However, many successful preparations of QDs/polymers by LBL, which were mostly based on quartz or spin-coating films as substrate, have been reported using QDs such as CdS-ZnS,[22] CdSe,[23] and CdTe.[24–26] There are sparse examples on the fabrication of luminescent electrospinning films using LBL.

Cellulose acetate (CA), a derivation of cellulose, can be easily obtained from natural resources.[27] Moreover, CA can be easily used to fabricate films with good mechanical properties.[28] In this article, luminescent electrospinning cellulose film was fabricated using LBL. For exposing more hydrophilic hydroxyl groups, CA nanofibrous mats were hydrolyzed with sodium hydroxide to remove acetyl groups. The thioglycolic acid (TGA) capped CdTe QDs, which have plenty of COO^- at the surface, are one of the most commonly used aqueous QDs because of high and stable luminescence.[29] Poly(diallyl dimethyl ammonium chloride) (PDDA) is a kind of polycation, which has many quaternary ammonium cations.[26]

Moreover, PDDA has good film-forming ability and susceptibility to chemical modifications.[30] The negatively charged TGA capped CdTe QDs can be attracted by positively charged PDDA. The fibrous mats decorated with CdTe QDs and PDDA had adjustable fluorescence intensity through altering the deposited bilayers. The approach presents a hopeful luminescence material for biosensors, light-emitting diodes, and other biomedical applications.

EXPERIMENTAL

Materials

Cadmium chloride, TGA, sodium tellurite, trisodium citrate, sodium borohydride, sodium hydroxide, N, N dimethyl acetamide, acetone and PDDA were purchased from Sinopharm Chemical Reagent Co., China. CA was obtained from Sigma-Aldrich. All other chemicals were of analytical grade without further purification. All aqueous solutions were prepared using ultrapure water with a resistance of 18.2 MΩ·cm.

Synthesis and Characterizations of Water-Soluble CdTe QDs

Water-soluble TGA capped CdTe QDs were synthesized by one-step method, with minor modification.[29] Briefly, 1.0×10^{-3} mol cadmium choride ($CdCl_2$) was dissolved in a 250-mL round bottom flake containing 100 mL ultrapure water with magnetic stirring. Then the solution turned to milky white after 1.2×10^{-3} mol TGA was added. The solution returned to transparent with adjusting the pH to 11. Finally, 1.5×10^{-3} mol trisodium citrate, 2.0×10^{-4} mol sodium tellurite, 9.6×10^{-4} mol sodium borohydride were added successively in the solution with continuous stirring. When the solution became slight green, the flask was connected to a condenser, refluxed at 100°C under ambient atmosphere from 10 min to 10 h. The obtained QDs were deposited with the same volume of alcohol, and centrifuged at 4000 r/min for 15 min in a refrigerated centrifuge (TGL-20000cR). The QDs precipitate was dried under nitrogen atmosphere, and redissolved in the same volume of ultrapure water. The optical properties of QDs were determined by RF-5301PC fluorescence spectrometer with 350 nm excitation wavelength and Shimadzu UV-1750 spectrophotometer. The morphology of QDs was observed on a TEM (H-7650, Hitachi, Japan). The fluorescence quantum yield of the QDs was calculated as given in Lovrić's report.[31]

Fabrication of CA Nanofibrous Mats and Their Hydrolysis

CA nanofibrous mats were fabricated by Deng's method.[32] The electrospinning solution was prepared by N, N dimethyl acetamide and acetone as mixed solvent (molar ratio was 2 : 1) contained 10% CA with continuous stirring for 12 h. Subsequently, the electrospinning process was performed at the following conditions: a flow rate of 1 mL/h, a working distance of 15 cm and an applied voltage of 15kV. The electrospun apparatus was equipped with an injector of 7 mm in diameter, a high-voltage power and an aluminum foil collector mounted on a steel stand. Typical experiments were carried out at a circumstance temperature of 20°C under ∼80% humidity. The CA fibrous mats were hydrolyzed by 0.05 mol/L sodium hydroxide for 7 days to regenerate cellulose.[33] Then the cellulose fibrous mats were washed with ultrapure water for several times, dried at 40°C and stored in a dryer for further usage.

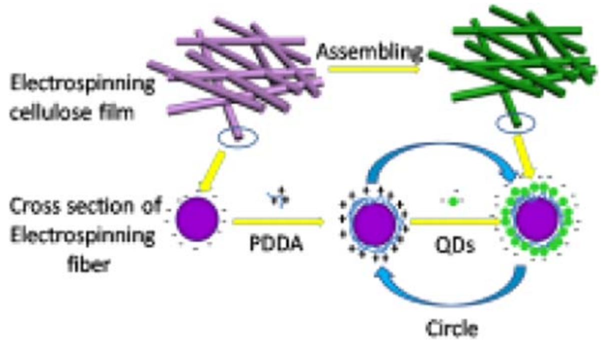

Figure 1. Schematic diagram illustrating the process of the LBL cellulose fibrous mat. [Color figure can be viewed in the online issue, which is available at wileyonlinelibrary.com.]

Formation of LBL Structured Multilayer on Cellulose Fibrous Mats

The concept for preparation of LBL structured fibrous mats was shows in Figure 1. Primary, cellulose fibrous mats were immersed into 1% PDDA solution for 20 min, and washed with ultrapure water for three times. Then, the mats were placed into CdTe quantum dots solution (3.5×10^{-5} M) for another 20 min, and washed again with distilled water for three times. That was a circle of 1 bilayer of QDs/PDDA deposition. By repeating the above operation, a series of cellulose fibrous mats were obtained with 2, 4, 6, 8, and 10 bilayers assemblies. Each of LBL deposited cellulose fibrous mat was coated with PDDA at the outside for reducing the oxidation of thiol groups on CdTe QDs. The $(QDs/PDDA)_n$ coated fibrous mats were dried at 40°C in vacuum and stored at 4°C.

Characterizations

The luminescent spectra were recorded on RF-5301PC fluorescence spectrometer at the same detecting condition of CdTe QDs. X-ray photoelectron spectroscopy (XPS) measurements were performed with VG Multilab 2000 X-ray Photoelectron Spectrometer. Fourier transform infrared spectroscopy (FTIR) measurements were recorded on NEXUS 470 spectrophotometer in the range of 4000–500 cm^{-1} at a resolution of 4 cm^{-1}, with air as the background. Differential scanning calorimetry (DSC) were performed with 204-F1 differential scanning calorimetry analyzer at a heating rate of 10°C/min under nitrogen atmosphere, at 50–400°C measuring temperature, 20 mL/min sweep gas and 60 mL/min protective gas. Thermogravimetric (TG) analysis was determined with TGA-20000 analyzer at the same heating rate of 10°C/min with nitrogen atmosphere at 30–400°C measuring temperatures. X-ray diffraction (XRD) measurements were performed with D/Max-IIIA XRD analyzer at a voltage of 30 kV, an electricity of 50 mA and a scanning rate of 4°/min. The morphology was studied by scanning electron microscope (SEM) with JSM-6700F at 15 kV and image resolution of 3.5 nm. Zeta potential was determined by using Zeta-Sizer Nano series (Nano-ZS, Malvern Instruments, Malvern, UK) at 633 nm with scattering angle of 173°.

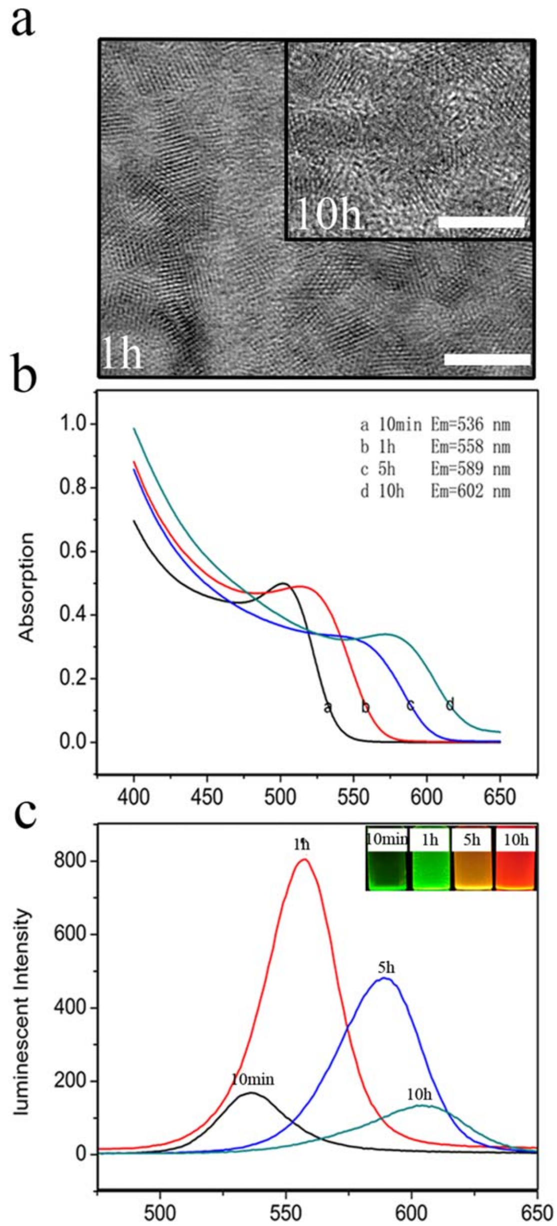

Figure 2. The optical properties and TEM images of CdTe QDs obtained at different heating time. (a) The TEM image of CdTe QDs obtained at the heating time of 1 and 10 h (scale bar 5 nm), (b) the visible spectroscopy of CdTe QDs obtained at different heating time from 10 min to 10 h, and (c) the luminescent intensities of CdTe QDs obtained at different heating time from 10 min to 10 h, the inset image was the photograph of CdTe QDs solutions under ultraviolet lamp. [Color figure can be viewed in the online issue, which is available at wileyonlinelibrary.com.]

RESULTS AND DISCUSSION

The Characterizations of CdTe QDs

The morphologies of CdTe QDs were observed by high resolution transmission electron microscopy [Figure 2(a,b)]. There were homogeneous distributions of CdTe QDs in TEM images. The average diameters of the QDs, which were obtained with reflux heating for 1 and 10 h, were 3.6 ± 0.15 nm and 4.2 ± 0.15 nm, respectively. This was mainly because of the Ostwald ripening process, in which smaller particles dissolve and large particles grow.[34] With reflux time prolonged, both the absorbance peak and luminescence emission peak became broad. It might be attributed that smaller particles dissolved in aqueous medium and the released monomers were consumed by the larger particles.[35] The UV–Vis absorption spectra and luminescence spectra [Figure 2(c,d)] were coincided with size-dependent quantum confinement effects, which were agreed with Sheng's report.[29] The luminescence intensity first significantly increased and then declined because the stabilizer decomposition with long time heating and producing the surface defect of the QDs.[35] The luminescent intensity of QDs which were gotten from heating for 1h reached the maximum, corresponding to the highest quantum yields (70.5%). The CdTe QDs of refluxing 1 h were employed in the following experiments.

Fabrication of LBL Films Coated Cellulose Fibrous Mats

The main driving force of LBL was the electrostatic interaction between template and the assembly layer. The cellulose nanofibrous mat and TGA coated CdTe QDs were negatively charged, and PDDA was positively charged. Based on this fact, the PDDA and QDs could be alternately deposited on the surface of cellulose mats through electrostatic interaction.[36] Figure 1 presents the process of LBL of PDDA and QDs, especially the ammonium groups of PDDA interacting with the carboxyl groups of QDs.

Surface Elemental Analysis of (QDs/PDDA)$_n$ Cellulose Mats

To verify the successful deposition of PDDA and QDs on the cellulose fibrous mat, XPS analysis was carried out to detect the surface elemental composition of the samples (Figure 3). The strong C 1s and O 1s peaks, which are the character of cellulose,[37,38] were observed in both the cellulose mat and (QDs/PDDA)$_{10}$ coated cellulose mat. Some extra peaks of N 1s (0.45%), Cd 3d (6.44%) and Te 3d (4.11%) were appeared in the (QDs/PDDA)$_{10}$ coated cellulose mats, confirming the deposition of PDDA and QDs.

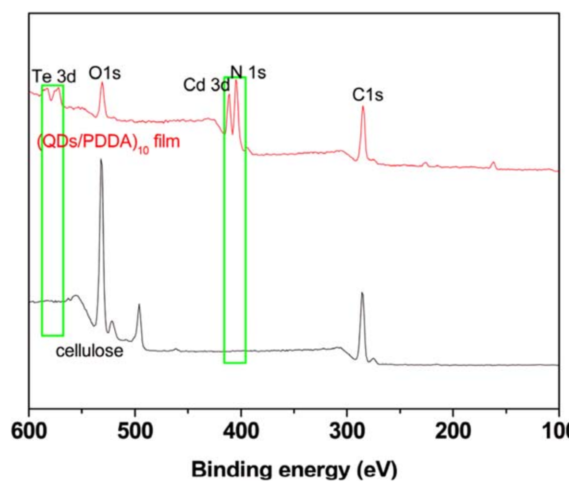

Figure 3. XPS analysis of cellulose and (QDs/PDDA)$_{10}$ cellulose fibrous mat. [Color figure can be viewed in the online issue, which is available at wileyonlinelibrary.com.]

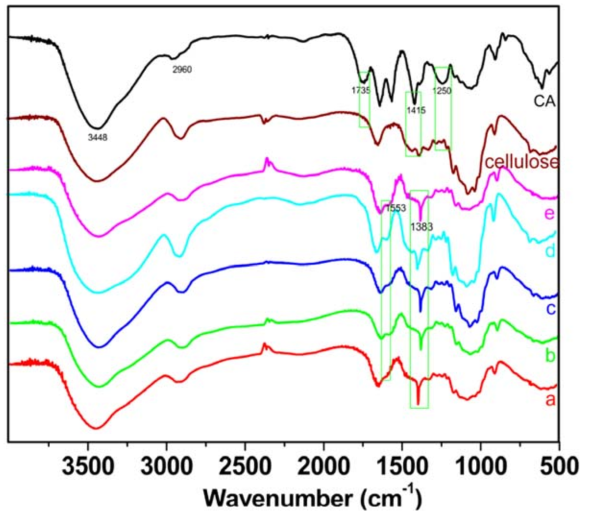

Figure 4. FTIR spectra: (a) $n = 2$, (b) $n = 4$, (c) $n = 6$, (d) $n = 8$, and (e) $n = 10$. [Color figure can be viewed in the online issue, which is available at wileyonlinelibrary.com.]

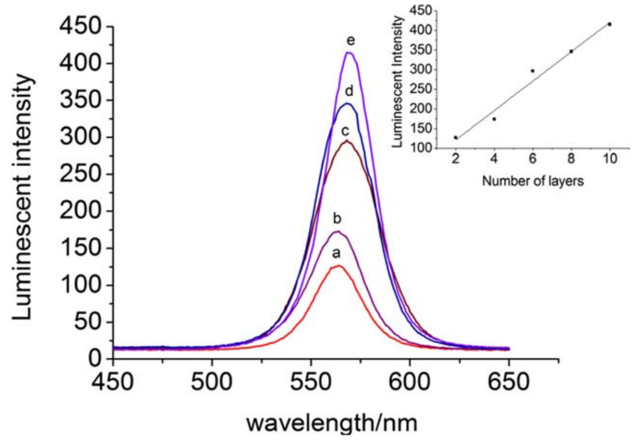

Figure 6. The fluorescent emission of $(QDs/PDDA)_n$ cellulose fibrous mat, the number of layers: (a) $n = 2$, (b) $n = 4$, (c) $n = 6$, (d) $n = 8$, and (e) $n = 10$. [Color figure can be viewed in the online issue, which is available at wileyonlinelibrary.com.]

FTIR Analysis of $(QDs/PDDA)_n$ Cellulose Mats

The infrared spectra of $(QDs/PDDA)_n$ cellulose mats were shown in Figure 4. For the spectrum of CA film, the featured peaks of acetate groups were observed at 1415 cm^{-1} ($V_{C\text{–}CH3}$), 1735 cm^{-1} ($V_{C=O}$), 1250 cm^{-1} ($V_{C\text{–}O\text{–}C}$), while for cellulose mat, the featured peaks of acetyl groups disappeared due to deacetylation with hydrolyzation.[39] At the same time, new peaks appeared at 1383 cm^{-1} (V_{CH3}) and 1553 cm^{-1} ($V_{N\text{–}H}$) in the spectra of $(QDs/PDDA)_n$ coated cellulose fibrous mats, which indicated the PDDA existed on the mats.

Morphology Analysis of $(QDs/PDDA)_n$ Cellulose Mats

SEM images of the fibrous mats coated with various bilayers of QDs and PDDA were obtained (Figure 5) to illustrate the evolution of surface morphologies during the LBL coating process. With the proceeding of LBL, the nanofibers showed a relatively higher surface roughness compared with the smooth surface of the cellulose [Figure 5(a–c)]. The roughness on the fibers was caused by the formation of QDs clusters, the dispersion speed of QDs and PDDA permeating into cellulose fibers.[40] Additionally, once the next layer was deposited, it would interpenetrate into the previously adsorbed layer. The slight crosslinking of the fibers appeared in Figure 5(b,c), was due to the mutual adsorption of the fibers during the process of LBL assembly.[40]

Luminescent Properties of $(QDs/PDDA)_n$ Cellulose Mats

Based on the optical properties of the QDs, the luminescent intensity of LBL coated cellulose mats could be monitored using fluorescent spectroscopy. The luminescence intensities of the QDs were gradually increased with adding the deposited bilayers (Figure 6). The luminescent growth trend was analyzed by plotting the values of emission peaks corresponding to the amount of bilayers (inset of Figure 6). A linear growth mode was found in this study ($R^2 = 0.97211$), which agreed well with growth mode of Constantine's result about QDs-based LBL films.[23] The results indicated that almost the equal amounts of QDs were adsorbed after each deposition cycle. However, the emission peaks were slightly red shifted when increasing the coated bilayers on the fibrous mats. This was probably due to the slight aggregation of CdTe QDs through the interaction of PDDA and CdTe QDs.[41]

Materials Crystallinity of the $(QDs/PDDA)_n$ Cellulose Mats

Figure 7 showed the XRD patterns of different cellulose fibrous mats. It can be seen that the cellulose mat exhibited a typical

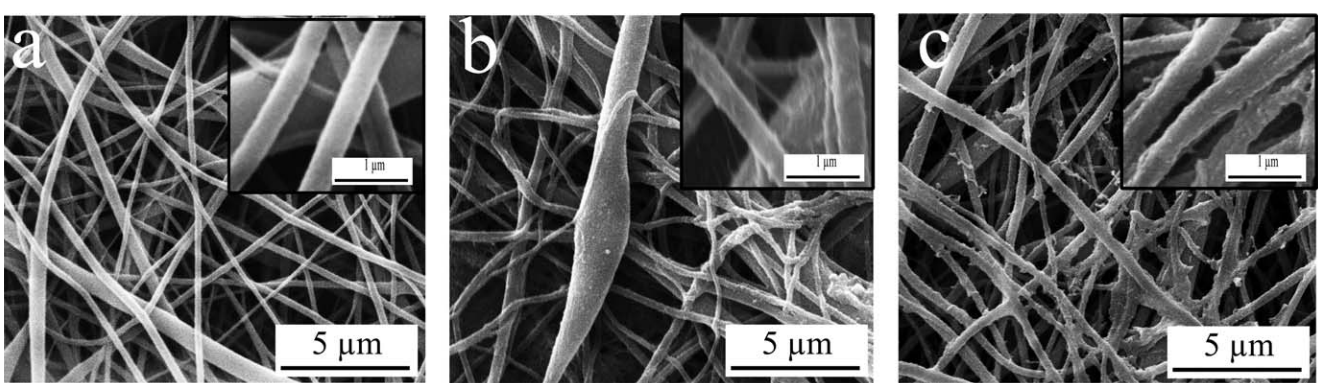

Figure 5. SEM images for nanofibrous mats: (a) cellulose fibrous mat, (b) $(QDs/PDDA)_5$ cellulose fibrous mat, and (c) $(QDs/PDDA)_{10}$ cellulose fibrous mat.

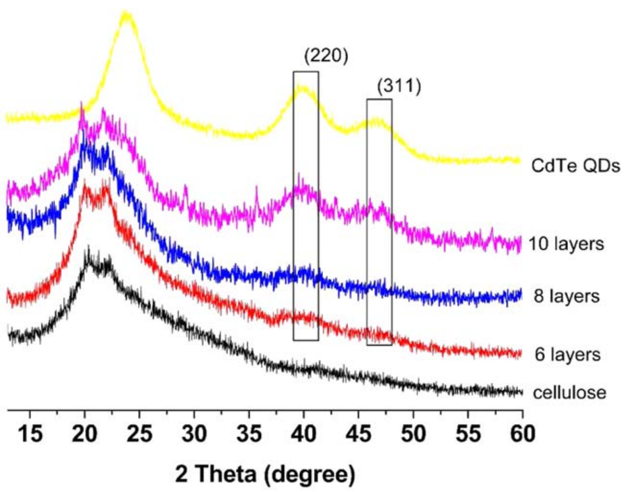

Figure 7. X-ray diffraction curves of cellulose and $(QDs/PDDA)_n$ cellulose fibrous mats. [Color figure can be viewed in the online issue, which is available at wileyonlinelibrary.com.]

cellulose II crystal with two characteristic diffraction peaks at 20.2° and 22.1°, which agreed with other reports.[39,42] Two small peaks appeared at 40° and 47° in $(QDs/PDDA)_6$ bilayers coated cellulose mat because the deposited amounts of QDs were too small to form agglomerates and the present very small amounts were not easily detected by XRD.[18] However, two distinct peaks appeared at the same degrees when the amounts of bilayers increased to 10. The results agreed with Li's report that the peaks of 220 and 311 crystal faces of cubic phase (zinc-blende) CdTe QDs were at 39° and 46°.[43]

Thermal Properties of $(QDs/PDDA)_n$ Cellulose Fibrous Mats

The thermal stability of $(QDs/PDDA)_n$ cellulose fibrous mats was evaluated by DSC and TG analysis. The samples displayed similar decomposition patterns with two main steps of weight loss in TG curves [Figure 8(a)]. The first weight loss from 0 to 200°C resulted from the evaporation of residual moisture and solvent, and the removal of low molecular weight molecules. Then, the second weight loss (from 200 to 370°C), plateaus around 370°C, is perhaps due to the decomposition of the mats.[44] It was observed that the decomposition of cellulose mat occurred at about 200°C. Besides, it could be seen that the decomposition temperatures of all LBL coated mats increased in the range of 250 and 300°C with the increasing of QDs/PDDA bilayers. The onset decomposition temperature was recorded to investigate the thermal stability of the mats.[36] The thermal stability of $(QDs/PDDA)_n$ cellulose mats were improved with increasing the deposited bilayers, possibly because of the free radical absorption by the QDs during the thermal decomposition of cellulose and retarding the mobility of the polymer, similar to other reports about QDs/polymer composite systems.[18,21]

The DSC analysis in Figure 8(b) was consistent with the TG results. The cellulose fibrous mat showed a broad exothermic event at about 200°C and a weak exothermic peak at 350°C which was associated with the degradation of the cellulose.[45] For $(QDs/PDDA)_n$ coated cellulose mats, the exothermic event at about 350°C might be attributed to the denaturation of PDDA. Furthermore, with increasing of the deposited layers, the exothermic peaks gradually shifted to higher temperature, which means the thermal stability also increased.

CONCLUSIONS

In summary, we investigated a photoluminescent cellulose fibrous mat coated by CdTe QDs and PDDA using LBL. It is retained the inherent physicochemical properties of CdTe QDs and cellulose during LBL deposited process. The luminescent intensity of the fibrous mats increased linearly with adding the assembled bilayers. Moreover, the deposition of QDs/PDDA could increase the thermal stability of cellulose mats. Therefore, the QDs/PDDA coated cellulose fibrous mat would be a prospective luminescence material which can be used as test paper, light emitting diode, and so on.

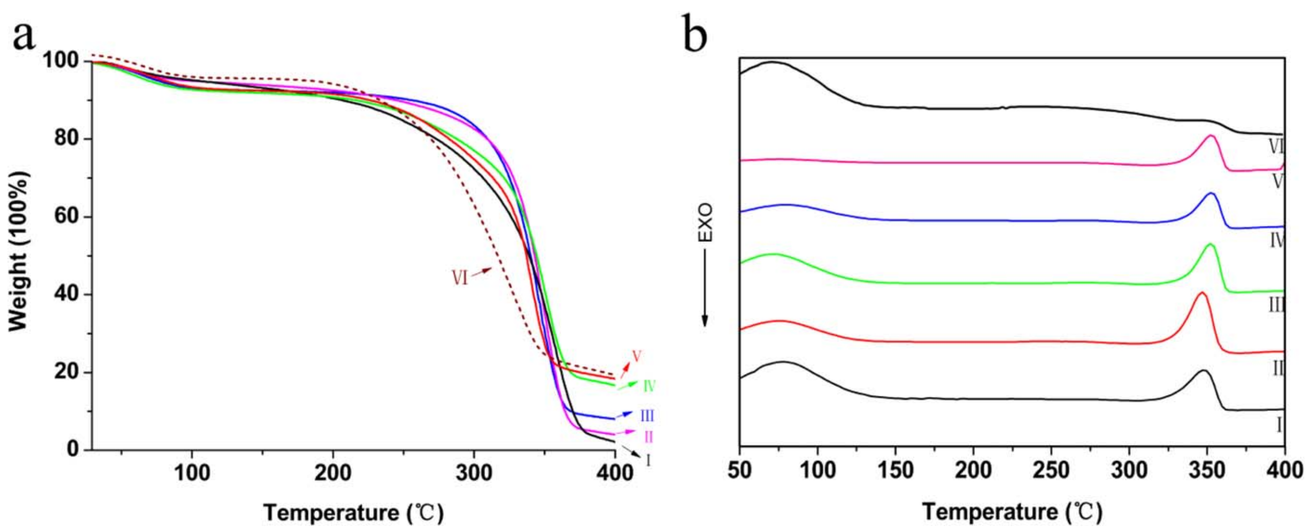

Figure 8. (a)TG curves for the $(QDs/PDDA)_n$ cellulose fibrous mats; (b) DSC Analysis of $(QDs/PDDA)_n$ cellulose fibrous mats. (I) $n = 2$, (II) $n = 4$, (III) $n = 6$, (IV) $n = 8$, (V) $n = 10$, and (VI) cellulose. [Color figure can be viewed in the online issue, which is available at wileyonlinelibrary.com.]

ACKNOWLEDGMENTS

This work was financially supported by the National Natural Science Foundation of China (Grant No. 31371841). We wish to thank colleagues of Key Laboratory of Environment Correlative Dietology of Huazhong Agricultural University for offering many conveniences of the experiments.

REFERENCES

1. Rakovich, A.; Donegan, J. F.; Oleinikov, V.; Molinari, M.; Sukhanova, A.; Nabiev, I.; Rakovich, Y. P. *J. Photochem. Photobiol. C-Photochem. Rev.* **2014**, *20*, 17.
2. Wu, P.; Yan, X.-P. *Chem. Soc. Rev.* **2013**, *42*, 5489.
3. Aboulaich, A.; Michalska, M.; Schneider, R.; Potdevin, A.; Deschamps, J.; Deloncle, R.; Chadeyron, G.; Mahiou, R. *ACS Appl. Mater. Interfaces* **2013**, *6*, 252.
4. Min, S.-Y.; Bang, J.; Park, J.; Lee, C.-L.; Lee, S. W.; Park, J.-J.; Jeong, U.; Kim, S.; Lee, T.-W. *RSC Adv.* **2014**, *4*, 11585.
5. Otto, T.; Müller, M.; Mundra, P.; V. Lesnyak; Demir, H. V.; Gaponik, N.; Eychmüller, *Nano Lett.* **2012**, *12*, 5348.
6. Liang, H.; Song, D.; Gong, J. *Biosens. Bioelectron.* **2014**, *53*, 363.
7. Costas-Mora, I.; Romero, V.; Lavilla, I.; Bendicho, C. *Trac-Trends Anal. Chem.* **2014**, *57*, 64.
8. Chen, L.-N.; Wang, J.; Li, W.-T.; Han, H.-Y. *Chem. Commun.* **2012**, *48*, 4971.
9. Jaque, D.; del Rosal, B.; Martin Rodriguez, E.; Martinez Maestro, L.; Haro-Gonzalez, P.; Garcia Sole, J. *Nanomedicine* **2014**, *9*, 1047.
10. Lia, J.; Zhu, J.-J. *Analyst* **2013**, *138*, 2506.
11. Yuan, J.; Gaponik, N.; Eychmüller, A. *Anal. Chem.* **2012**, *84*, 5047.
12. Gordillo, H.; Suarez, I.; Abargues, R.; Rodriguez-Canto, P.; Albert, S.; Martinez-Pastor, J. P. *J. Nanomater.* **2012**, dx.doi.org/10.1155/2012/960201.
13. Frigerio, C.; Ribeiro, D. S. M.; Rodrigues, S. S. M.; Abreu, V. L. R. G.; Barbosa, J. A. C.; Prior, J. A. V.; Marques, K. L.; Santos, J. L. M. *Anal. Chim. Acta* **2012**, *735*, 9.
14. Antony, J. V.; Kurian, P.; Vadakkedathu, N. P.; Kochimoolayil, G. E. *Ind. Eng. Chem. Res.* **2014**, *53*, 2261.
15. Goncalves, L.; Kanodarwala, F. K.; Stride, J. A.; Silva, C. J. R.; Gomes, M. J. M. *Opt. Mater.* **2013**, *36*, 186.
16. Abitbol, T.; Wilson, J. T.; Gray, D. G. *J. Appl. Polym. Sci.* **2011**, *119*, 803.
17. Zhu, J.; Wei, S.; Patil, R.; Rutman, D.; Kucknoor, A. S.; Wang, A.; Guo, Z. *Polymer* **2011**, *52*, 1954.
18. Mthethwa, T. P.; Moloto, M. J.; De Vriesand, A.; Matabola, K. P. *Mater. Res. Bull.* **2011**, *46*, 569.
19. Kumar, H.; Srivastava, R.; Dutta, P. *Carbohydr. Polym.* **2013**, *97*, 327.
20. Zhang, Y. W.; Zhuang, S. D.; Xu, X. Y.; Hu, J. G. *Opt. Mater.* **2013**, *36*, 169.
21. Wei, S.; Sampathi, J.; Guo, Z.; Anumandla, N.; Rutman, D.; Kucknoor, A.; James, L.; Wang, A. *Polymer* **2011**, *52*, 5817.
22. Kim, D.; Okahara, S.; Shimura, K.; Nakayama, M. *J. Phys. Chem. C* **2009**, *113*, 7015.
23. Constantine, C. A.; Gattás-Asfura, K. M.; Mello, S. V.; Crespo, G.; Rastogi, V.; Cheng, T.-C.; DeFrank, J. J.; Leblanc, R. M. *J. Phys. Chem. B* **2003**, *107*, 13762.
24. Li, X.; Luand, Z.; Li, Q. *Thin Solid Films* **2013**, *548*, 336.
25. Liu, M.; Zhao, H.; Chen, S.; Wang, H.; Quan, X. *Inorg. Chim. Acta* **2012**, *392*, 236.
26. Wang, C.; Zhao, J.; Wang, Y.; Lou, N.; Ma, Q.; Su, X. *Sens. Actuators B: Chem.* **2009**, *139*, 476.
27. Li, W.; Li, X.; Li, W.; Wang, T.; Li, X.; Pan, S.; Deng, H. *Eur. Polym. J.* **2012**, *48*, 1846.
28. Huang, W.; Xu, H.; Xue, Y.; Huang, R.; Deng, H.; Pan, S. *Food Res. Int.* **2012**, *48*, 784.
29. Sheng, Z.; Han, H.; Hu, X.; Chi, C. *Dalton Trans.* **2010**, *39*, 7017.
30. Jie, G.; Li, L.; Chen, C.; Xuan, J.; Zhu, J.-J. *Biosens. Bioelectron.* **2009**, *24*, 3352.
31. Lovrić, J.; Bazzi, H. S.; Cuie, Y.; Fortin, G. R.; Winnik, F. M.; Maysinger, D. *J. Mol. Med.* **2005**, *83*, 377.
32. Deng, H.; Wang, X.; Liu, P.; Ding, B.; Du, Y.; Li, G.; Hu, X.; Yang, J. *Carbohydr. Polym.* **2011**, *83*, 239.
33. Lu, P.; Hsieh, Y.-L. *J. Membr. Sci.* **2010**, *348*, 21.
34. Li, Z.; Dong, C.; Tang, L.; Zhu, X.; Chen, H.; Ren, J. *Luminescence* **2011**, *26*, 439.
35. Zhu, Y.; Li, C.; Xu, Y.; Wang, D.; J. *Alloys Compd.* **2014**, *608*, 141.
36. Zhou, B.; Hu, Y.; Li, J.; Li, B. *Int. J. Biol. Macromol.* **2014**, *64*, 402.
37. Son, W. K.; Youk, J. H.; Lee, T. S.; Park, W. H. *Macromol. Rapid Commun.* **2004**, *25*, 1632.
38. Li, W.; Li, X.; Wang, Q.; Pan, Y.; Wang, T.; Wang, H.; Song, R.; Deng, H. *Carbohydr. Polym.* **2014**, *99*, 218.
39. Yu, S.; Cheng, Q.; Huang, C.; Liu, J.; Peng, X.; Liu, M.; Gao, C. *J. Membr. Sci.* **2013**, *434*, 44.
40. Deng, H.; Zhou, X.; Wang, X.; Zhang, C.; Ding, B.; Zhang, Q.; Du, Y. *Carbohydr. Polym.* **2010**, *80*, 474.
41. Li, M.; Zhang, J.; Zhang, H.; Liu, Y.; Wang, C.; Xu, X.; Tang, Y.; Yang, B. *Adv. Funct. Mater.* **2007**, *17*, 3650.
42. Zhou, B.; Li, Y.; Deng, H.; Hu, Y.; Li, B. *Colloids Surf. B: Biointerfaces* **2014**, *116*, 432.
43. Li, Q.; Chi, K.; Mu, Y.; Zhang, W.; Yang, H.; Fu, W.; Zhou, L. *Mater. Lett.* **2014**, *117*, 225.
44. Lucena, M. d. C. C.; de Alencar, A. E. V.; Mazzeto, S. E.; Soares, S. d. A. *Polym. Degrad. Stabil.* **2003**, *80*, 149.
45. Liu, H.; Hsieh, Y. L. *J. Polym. Sci. Part B: Polym. Phys.* **2002**, *40*, 2119.